

Entropy theory for movement of moisture in soils

Vijay P. Singh¹

Received 11 June 2009; revised 7 October 2009; accepted 28 October 2009; published 13 March 2010.

[1] An entropy theory is formulated for one-dimensional movement of moisture in unsaturated soils in the vertically downward direction. The theory is composed of five parts: (1) Tsallis entropy, (2) principle of maximum entropy, (3) specification of information on soil moisture in terms of constraints, (4) maximization of the Tsallis entropy, and (5) derivation of the probability distributions of soil moisture. The theory is applied to determine the soil moisture profile under three conditions: (1) the moisture is maximum at the soil surface and decreases downward to a minimum value at the bottom of the soil column (it may be near the water table); (2) the moisture is minimum at the soil surface and increases downward to a maximum value at the end of the soil column (this case is the opposite of case 1); and (3) the moisture at the soil surface is low and increases downward up to a distance and then decreases up to the bottom (this case combines case 2 and case 1). The entropy-based soil moisture profiles are tested using experimental observations reported in the literature, and properties of these profiles are enumerated.

Citation: Singh, V. P. (2010), Entropy theory for movement of moisture in soils, *Water Resour. Res.*, 46, W03516, doi:10.1029/2009WR008288.

1. Introduction

[2] Soil moisture occupies a central position in the hydrologic cycle, interfacing between land surface hydrologic processes and atmosphere on one hand and between land surface processes and lithosphere (groundwater zone) on the other hand. The zone of soil moisture (also called vadose zone) is often called the gate keeper in hydrology. Soil moisture is fundamental to analysis and evaluation of soil erosion, droughts, generation of runoff, irrigation scheduling and management, maintaining salt balance and reducing water logging, tactical military encampment and mobility, determination of evapotranspiration, sustaining ecological health, and spread of bacterial and viral activities. Because of its ubiquitous use, recent years have witnessed considerable emphasis on measurement of soil moisture using, as for example, neutron probes, TDR probes, and remote sensing techniques. In the case of remote sensing, soil moisture estimates are obtained within a depth of no more than 5 cm [Ulaby *et al.*, 1996] and modeling methods are needed to estimate the entire soil moisture profile.

[3] The soil moisture profile using near-surface soil moisture observations has been estimated using a range of approaches [Schmugge *et al.*, 1980] which can be grouped into (1) theoretical [Russo, 1988], (2) probabilistic [Assouline *et al.*, 1998], (3) water balance [Singh, 1989], (4) regression [Arya *et al.*, 1983], (5) inverse [Kostov and Jackson, 1993], and (6) intelligence [Koekkoek and Booltink, 1999]. Theoretical approaches include solution of equations governing flow of water in soils. The solution, of course, requires the

knowledge of soil hydraulic characteristics, including a hydraulic conductivity function and a water retention function which needs to be determined. Thus, in this sense this becomes an inverse problem. In probabilistic techniques, the soil structure is hypothesized to evolve from a random fragmentation process. Assouline *et al.* [1998] have presented a conceptual model using a probabilistic approach in which the fragmentation process leads to the determination of the soil particle size distribution. Particle volumes are converted into pore volumes using a power function. Then, a capillarity equation is employed to obtain an expression for the water retention curve. Or *et al.* [2000] developed a stochastic model coupling the probabilistic nature of pore space distributions with physically based soil deformations employing the Fokker-Planck equation. They addressed three features of pore space evolution: reduction of total porosity, reduction of mean pore radius, and changes in the variance of pore size distribution. This model permits computation of temporal variation of near-surface soil hydraulic properties. Using the Shannon entropy Al-Hamdan and Cruise [2010] derived soil moisture profiles. Although they did not discuss the probabilistic attributes of their methodology and of soil moisture profiles, their approach is probabilistic. Pachepsky *et al.* [2006] employed information theory measures to compare and evaluate different soil water models.

[4] The water balance approach incorporates soil moisture as the output in the water balance [De Troch *et al.*, 1996]. This approach entails modeling infiltration, including redistribution and reinfiltration [Melone *et al.*, 2006]. In recent years soil moisture observations have been assimilated into hydrologic models [Das and Mohanty, 2006] and integrating soil moisture observations with hydrologic models seems a more promising approach [Kostov and Jackson, 1993]. Regression techniques are curve fitting, relating near-surface soil moisture observations to wetting and drying separately at specific locations. For shallow depths Arya *et al.* [1983],

¹Department of Biological and Agricultural Engineering and Department of Civil and Environmental Engineering, Texas A&M University, College Station, Texas, USA.

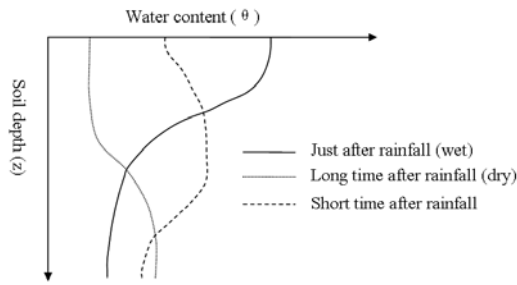


Figure 1. Moisture distribution in three phases.

Bruckler *et al.* [1988], Srivastava *et al.* [1997], among others, found regression techniques to yield satisfactory estimates, but the development of regression relations needs sufficient observations at each location and that these relations cannot be transferred to other locations.

[5] In the inverse approaches, since the microwave brightness temperature profile is estimated from soil moisture estimates, using an inverse technique remotely sensed brightness temperature can be employed for estimating soil moisture [Kostov and Jackson, 1993]. Intelligence techniques are based on artificial neural networks [Koekkoek and Booltink, 1999; Jain *et al.*, 2004], genetic algorithms, fuzzy logic, artificial intelligence, and the like. Using a priori information on the hydrologic properties of soils, soil moisture content is determined at different depths. Methods of determination include correlations between surface soil moisture and that at lower layers [Kondratyev *et al.*, 1977], or energy based methods with radiative properties of soil at different soil moisture states [Reutov and Shutko, 1986], or models using hydrostatic principles [Jackson *et al.*, 1987].

[6] This review suggests that although the Shannon entropy was used by Pachepsky *et al.* [2006] and Al-Hamdan and Cruise [2010], the Tsallis entropy has not been employed for describing the movement of soil moisture thus far. It may be interesting to explore the use of the Tsallis entropy for soil moisture modeling, for it possesses a number of interesting properties and encompasses the Shannon entropy as a special case. The objective of this study, therefore, is to develop an entropy theory using the Tsallis entropy for describing the one-dimensional movement of soil moisture in unsaturated soils, and test the theory using experimental observations reported in the hydrologic literature. The theory permits a probabilistic description of soil moisture. The paper is organized as follows. Introducing the problem of soil moisture movement and estimation in this section, the soil moisture zone or vadose zone is described in section 2. The entropy theory is developed in section 3, and application of the theory is illustrated by deriving soil moisture profiles in section 4. The theory is tested in section 5, followed by conclusions in section 6.

2. Soil Moisture Zone

[7] The porous medium below the land surface can be divided into two zones: one between the water table and the land surface, and the other below the water table. The water table is defined as the surface on which the fluid pressure in the pores of a medium is exactly atmospheric. This means that the hydraulic head at any point on the water table must

equal the elevation of the water table at that point. The porous medium below the water table is saturated, i.e., the pores are filled with water, and can be referred to as groundwater or saturated geologic zone. The porous medium above the water table is often divided into three zones: (1) capillary fringe, (2) intermediate zone, and (3) soil moisture zone (also called root zone). There exists a narrow zone immediately above the water table, called capillary zone or fringe, where the porous medium is tension saturated but the pressure head is negative. This zone is also called tension-saturated zone. This pressure is the air entry pressure or bubbling pressure. The medium above the capillary fringe is called unsaturated zone or vadose zone or zone of aeration. In this zone, pores are partially filled with water, and partially filled with air. This means that water in the soil pores is under surface tension forces and thus the pressure will be negative. In this zone both the moisture content (θ) and the hydraulic conductivity (K) are functions of the pressure head (ψ). Furthermore, the θ - ψ relationship is hysteretic and the same is true of the K - ψ relationship. This means that these relationships during wetting are somewhat different from those during drying. From an agricultural standpoint, the vadose zone can be further divided into two zones. The zone below the land surface is the zone in which agricultural crops grow and it may thus be called root zone. This is also referred to as soil moisture zone. Below this zone is intermediate zone or percolation zone or transmission zone.

[8] When water is applied to the land surface either artificially by irrigation or naturally by rainfall, part of this water infiltrates the soil, depending, of course, upon soil characteristics, soil treatment, vegetation, and antecedent soil moisture condition. The movement of moisture upon entry at the surface will depend on the duration for which water is applied at the surface and the moisture existing beforehand. The soil surface will first get saturated at the surface and the saturated zone will move downward until it reaches the water table. This case, labeled as case 1, is called the wetting phase. In this case the distribution of soil moisture is monotonically decreasing from the surface to the water table or up to a point of concern. When the supply of water is cut off, the downward movement of moisture will continue and the soil will start draining. This case, labeled as case 2, is called the drying phase. In this case the distribution of moisture is monotonically increasing downward. Between these two phases there exists a situation where the distribution of moisture is monotonically increasing downward up to a point (zone one) but then decreasing downward (zone two). In this case, labeled as case 3, one can divide the unsaturated zone into these two zones. The three cases are shown in Figure 1.

3. Development of Entropy Theory

[9] Consider a soil column of length L . The moisture in this soil column can vary from a very low-value Θ_0 to the soil porosity n . Let the effective saturation θ be defined as

$$\theta = \frac{\Theta - \Theta_0}{n - \Theta_0} \quad (1)$$

where Θ is the moisture content, Θ_0 is the initial moisture content or the moisture content that cannot be extracted by

plants, and n is porosity. It is assumed that all values of soil depth z are equally likely between 0 and L corresponding to a given θ , and all values of θ are equally likely at any value of z , $\theta(z)$. Thus, the effective saturation is considered as a random variable with probability density function as $f(\theta)$ which is determined using the entropy theory.

[10] For determining the movement of moisture, an entropy theory is formulated as comprising five parts: (1) Tsallis entropy, (2) principle of maximum entropy (POME), (3) specification of constraints for the maximization of the Tsallis entropy in accord with POME, (4) maximization of entropy, and (5) determination of least biased probability distributions of soil moisture and maximum entropy. The theory is employed to derive soil moisture profiles for the aforementioned cases.

3.1. Tsallis Entropy

[11] Nearly two decades ago, *Tsallis* [1988] introduced what is now referred to as the Tsallis entropy, which can be expressed as

$$H(\theta) = \frac{k}{m-1} \left[1 - \int_a^b (f(\theta))^m d\theta \right] \\ = \frac{k}{m-1} \int_a^b f(\theta) \{1 - [f(\theta)]^{m-1}\} d\theta \quad (2)$$

where m is a real number, k is a conventional positive constant (needed to keep the units of H consistent) taken as unity without loss of generality, and a and b are lower and upper limits of θ . H describes the uncertainty associated with $f(\theta)$ and in turn θ . If $\{1 - [f(\theta)]^{m-1}\}/(m-1)$ is considered as a measure of uncertainty, then equation (2) represents the average uncertainty of θ . More the uncertainty more information will be needed to characterize θ . In this sense, information and uncertainty are related. Thus, the key in equation (2) is to derive the least biased $f(\theta)$.

[12] Before proceeding further, it may be useful to review the Tsallis entropy here. The Tsallis entropy is a non-extensive entropy and reduces to the Shannon entropy if exponent m in equation (2) is unity. It can also be said that for $m \rightarrow 1$, equation (2) reduces to the Boltzmann-Gibbs statistics. H is maximum for all values of m in the case of equiprobability. H is maximum if $m > 0$ and is minimum if $m < 0$. Like the Shannon entropy, the Tsallis entropy satisfies the additivity property for independent systems. Because of these and other properties, the Tsallis entropy has received and continues to receive a great deal of attention, especially in physics. It has been applied to describe a variety of thermodynamical systems with long-range interactions or memory and with fractal or multifractal boundary conditions, including turbulence, fractility and nonextensivity, scaling, anomalous diffusion, and complexity. *Tsallis* [2004] provided a comprehensive review of the construction and physical interpretation of nonextensive statistical mechanics, with particular reference to the Tsallis entropy. In 2005 European Physical Society published a special issue of *Europhysics News* on Nonextensive Statistical Mechanics: New Trends and perspective, in which a number of articles deal with different aspects and applications of the Tsallis entropy [*Boon and Tsallis*, 2005]. In a review of non-

extensive statistical mechanics and thermodynamics, *Tsallis* [2002] explored the possibility of using $m-1$ (entropic nonextensivity) as a measure of complexity for some classes of systems exemplified as above and high-energy collisions, solar neutrino problem, and so on.

[13] *Boghosian* [1996] presented the construction of a comprehensive thermodynamic description of two dimensional turbulence. He noted that two-dimensional Euler turbulence and drift turbulence did not maximize the Boltzmann entropy but the maximization of the Tsallis entropy was capable of explaining this phenomenon. *Gotoh and Kraichnan* [2004] critically examined the applicability of the Tsallis entropy to turbulence. *Arimitsu and Arimitsu* [2002a, 2002b] derived the probability density function of velocity fluctuation with the multifractal aspect in fully developed turbulence. Non-Gibbsian statistics are being observed these days in various fields and with the aid of the Tsallis entropy, they were able to obtain an abstract statistical mechanics.

[14] *Costa et al.* [1997] provided the microscopic interpretation of the entropic index m characterizing non-extensive statistics. They showed that a fractal subset of the phase space within which the system is driven by its own dynamics determines m . They investigated the power law sensitivity to initial conditions within a logistic-like map, and derived the relation between m and fractal dimension of the onset-to-chaos attractor. Extending the results of this study, *Lyra and Tsallis* [1998] provided general scaling arguments and showed that proper nonextensive statistics can be inferred from the scaling properties of the dynamical attractor at the start of chaos in one-dimensional dissipative maps. At the self-organized critical state *Papa and Tsallis* [1998] showed a power law sensitivity in the system of competing logistic maps.

[15] The Boltzmann-Gibbs statistics is not capable of dealing with anomalous diffusion which plays a fundamental role in the dynamics of a wide class of systems, such as turbulent flows, phase space motion in chaotic dynamics, and transport in highly heterogeneous materials. Anomalous diffusion is controlled by Levy distributions. *Zanette and Alemany* [1995] have pointed out that the Tsallis entropy is a natural tool for constructing a thermodynamic formalism of the anomalous diffusion. They then computed the mean square displacement as a function of time and generalized the Einstein relation of diffusivity and temperature for random walks of the Levy flight type. *Tsallis and Bukman* [1996] derived exact time-dependent solutions and their thermostatical basis for anomalous diffusion. *Prato and Tsallis* [1999] developed a nonextensive foundation of Levy distributions. Indeed they showed that nonextensive statistical mechanics, formulated in terms of m -expectation values, unifies the foundations of both the Gaussian and Levy distributions.

[16] These applications have been primarily in physics, although many of them relate to hydrological processes and will therefore have relevance in hydrological analysis and modeling. *Koutsoyiannis* [2005a, 2005b] was the first to employ the Tsallis entropy to characterize stochastic behavior of hydrological processes. *Keylock* [2005] introduced the Tsallis entropy and m -exponential distribution for deriving flood recurrence intervals. He reasoned that a distribution derived from power law considerations would be more appropriate than the power law itself. Hence it can

be argued that the nonextensive statistical mechanics has potential for much broader application in hydrology than is presented in this study.

3.2. Principle of Maximum Entropy

[17] The principle of maximum entropy formulated by Jaynes [1957a, 1957b] says that the least biased probability distribution of θ , $f(\theta)$, will be the one that will maximize equation (2), subject to the given information on θ expressed as constraints. In other words, if no information other than the given constraints is available then the probability distribution should be selected such that it is least biased toward what is not known. Such a probability distribution is yielded by the maximization of the Tsallis entropy. Thus, one of the key points is to define constraints on θ .

3.3. Specification of Constraints

[18] Information on θ can be obtained using the knowledge of soil physics and experimental observations. For a given soil, one may measure soil moisture at different depths and describe its characteristics. If soil moisture observations are available, then one way to express information on the soil moisture $\theta(z)$ is in terms of constraints C_r , $r = 0, 1, 2, \dots, n$, defined as

$$C_0 = \int_a^b f(\theta) d\theta = 1 \quad (3a)$$

$$C_r = \int_a^b g_r(\theta) f(\theta) d\theta = \overline{g_r(\theta)}, \quad r = 1, 2, \dots, n \quad (3b)$$

where $g_r(\theta)$, $r = 1, 2, \dots, n$, represent some functions of θ , a is the lower limit of θ , and b is the upper limit of θ , n denotes the number of constraints, and $\overline{g_r(\theta)}$ is the expectation of $g_r(\theta)$. If, for example, $r = 1$ and $g_1(\theta) = \theta$, equation (3b) would correspond to the mean effective saturation $= \bar{\theta}$; likewise, for $r = 2$ and $g_2(\theta) = (\theta - \bar{\theta})^2$ equation (3b) would denote the variance of θ . For most moisture profiles, more than two constraints are not needed. Tsallis *et al.* [1998] examined the role of constraints for the Tsallis entropy and their consequences for various systems. The constraints can be expressed in two ways: (1) in an ordinary manner used as above in equations (3a) and (3b) and (2) in power form involving $[f(\theta)]^m$. Abe and Bagci [2005] examined these two ways of choosing constraints and showed that both of them lead to the maximum Tsallis entropy distributions of a similar type, but the second way is connected to the generalized relative entropy. However, S. Abe (Instability of q-expectation value, 2008, available at arXiv:0806.3934v1) showed that the m -expectation value is not stable under small changes of a probability distribution, whereas the ordinary expectation value is. This subject needs further scrutiny for problems in hydrology and is beyond the scope of this study. For this study we chose the first way for purposes of simplicity.

3.4. Maximization of the Tsallis Entropy

[19] In order to obtain the least biased $f(\theta)$, the entropy given by equation (2) is maximized, subject to equations (3a) and (3b), and one simple way to achieve the maximization is

the use of the method of Lagrange multipliers. To that end, the Lagrangian function L can be constructed as

$$L = \frac{1}{m-1} \int_a^b f(\theta) \{1 - [f(\theta)]^{m-1}\} d\theta + \lambda_0 \left[\int_a^b f(\theta) d\theta - C_0 \right] + \sum_{r=1}^n \lambda_r \left[\int_a^b f(\theta) g_r(\theta) d\theta - C_r \right] \quad (4a)$$

where $\lambda_1, \lambda_2, \dots, \lambda_n$ are Lagrange multipliers. In order to obtain $f(\theta)$ which maximizes L , one may recall the Euler-Lagrange equation of the calculus of variation, and therefore one differentiates L with respect to $f(\theta)$ [noting θ as parameter and f as variable] and equates the derivative to zero and obtains

$$\frac{\partial L}{\partial f} = 0 \Rightarrow \frac{1}{m-1} \left\{ (1 - [f(\theta)]^{m-1}) - (m-1)[f(\theta)]^{m-1} \right\} + \lambda_0 + \sum_{r=1}^n \lambda_r g_r(\theta) = 0 \quad (4b)$$

3.5. Probability Distribution and Entropy of Soil Moisture

[20] Equation (4b) leads to the probability density function of θ in terms of the given constraints:

$$f(\theta) = \left\{ \frac{m-1}{m} \left[\frac{1}{m-1} + \lambda_0 + \sum_{r=1}^n \lambda_r g_r(\theta) \right] \right\}^{\frac{1}{m-1}} \quad (5a)$$

where λ_r 's are Lagrange multipliers which can be determined with the use of equations (3a) and (3b). Integration of equation (5a) leads to the cumulative distribution function or simply probability distribution of θ , $F(\theta)$:

$$F(\theta) = \int_a^\theta \left\{ \frac{m-1}{m} \left[\frac{1}{m-1} + \lambda_0 + \sum_{r=1}^n \lambda_r g_r(\theta) \right] \right\}^{\frac{1}{m-1}} d\theta \quad (5b)$$

[21] Substitution of equation (5a) in equation (2) results in the maximum entropy of $f(\theta)$ or θ :

$$H = \frac{1}{m-1} \int_a^b \left\{ \frac{m-1}{m} \left[\frac{1}{m-1} + \lambda_0 + \sum_{r=1}^n \lambda_r g_r(\theta) \right] \right\}^{\frac{1}{m-1}} \cdot \left[1 - \left\{ \frac{m-1}{m} \left[\frac{1}{m-1} + \lambda_0 + \sum_{r=1}^n \lambda_r g_r(\theta) \right] \right\} \right] d\theta \quad (6)$$

Equation (6) shows that the entropy of the probability distribution of $f(\theta)$ or θ depends only on the constraints, since the Lagrange multipliers themselves can be expressed in terms of the specified constraints. Equations (2), (3a), (3b), (5a), and (6) constitute the building blocks of the entropy theory.

4. Derivation of Soil Moisture Profiles

[22] Now the entropy theory is applied to the derivation of soil moisture profiles for the aforementioned three cases.

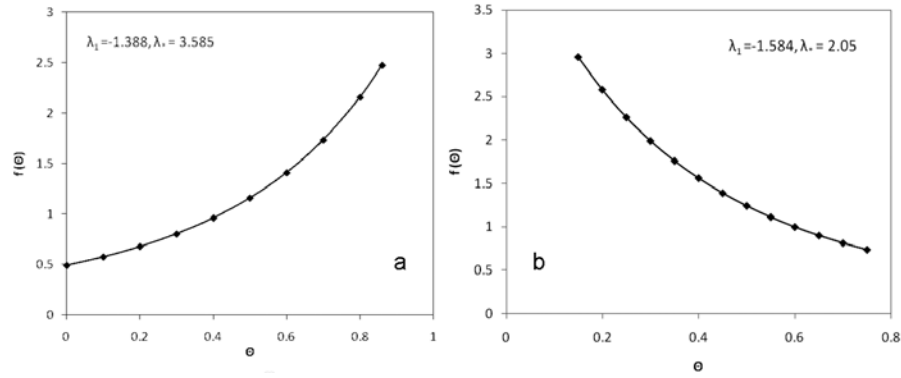


Figure 2. Probability density functions: (a) wet case and (b) dry case.

To that end, a fundamental hypothesis is employed. This hypothesis states that the cumulative probability distribution of θ is a linear function of z and its specific form will depend on the case under consideration.

4.1. Case 1: Wet Case

[23] This case occurs during and immediately after rain-fall or application of water at the soil surface and is designated as wet case. The moisture content is highest near the surface and decreases downward.

4.1.1. Formulation of Hypothesis

[24] It is hypothesized that the cumulative probability distribution function of θ can be expressed as

$$F(\theta) = 1 - \frac{z}{L}, \quad f(\theta) = -\frac{1}{L} \frac{dz}{d\theta} \quad (7)$$

4.1.2. Specification of Constraints

[25] In order to derive the moisture content profile using the entropy theory, the following constraints are defined:

$$\int_{\theta_L}^{\theta_u} f(\theta) d\theta = 1 \quad (8a)$$

$$\int_{\theta_L}^{\theta_u} \theta f(\theta) d\theta = \bar{\theta} \quad (8b)$$

where θ_L and θ_u are the values of the effective saturation at $z = L$ and $z = 0$, respectively.

4.1.3. Maximization of Entropy

[26] Applying POME and the method of Lagrange multipliers, one constructs the Lagrangian functions L as:

$$L = \int_{\theta_L}^{\theta_u} \frac{f(\theta)}{m-1} \left\{ 1 - [f(\theta)]^{m-1} \right\} d\theta + \lambda_0 \left[\int_{\theta_L}^{\theta_u} f(\theta) d\theta - 1 \right] + \lambda_1 \left[\int_{\theta_L}^{\theta_u} \theta f(\theta) d\theta - \bar{\theta} \right] \quad (9a)$$

where λ_0 and λ_1 are Lagrange multipliers. Differentiating equation (9a) with respect to $f(\theta)$ and equating the derivative

to 0 while recalling the Euler-Lagrange equation of the calculus of variation, one obtains

$$\frac{\partial L}{\partial f(\theta)} \Rightarrow 0 = \frac{1}{m-1} \left[\left\{ 1 - [f(\theta)]^{m-1} \right\} - (m-1)[f(\theta)]^{m-1} \right] + \lambda_0 + \lambda_1 \theta \quad (9b)$$

4.1.4. Probability Density Function

[27] Equation (9b) results in the probability density function of θ as

$$f(\theta) = \left\{ \frac{m-1}{m} \left[\frac{1}{m-1} + \lambda_0 + \lambda_1 \theta \right] \right\}^{\frac{1}{m-1}} \quad (10)$$

Equation (10) contains the Lagrange multipliers λ_0 and λ_1 which are determined using equations (8a) and (8b). For simplicity, one may write: $\lambda_* = \lambda_0 + \frac{1}{m-1}$. Then, equation (10) becomes

$$f(\theta) = \left\{ \frac{m-1}{m} [\lambda_* + \lambda_1 \theta] \right\}^{\frac{1}{m-1}} \quad (11)$$

The probability density function of soil moisture content, given by equation (11), is shown in Figure 2a for a wet case. It increases from a finite value and takes on a shape which is concave to the θ axis.

4.1.5. Maximum Entropy

[28] Using equation (10) in equation (2), one obtains the maximum entropy as

$$H = \frac{1}{m-1} - \frac{1}{m} \left(\frac{1}{m-1} + \lambda_0 + \lambda_1 \bar{\theta} \right) \quad (12a)$$

or with the use of equation (11) in equation (2), the maximum entropy can be written as

$$H = \frac{1}{m-1} - \frac{1}{m} (\lambda_* + \lambda_1 \bar{\theta}) \quad (12b)$$

4.1.6. Determination of Lagrange Multipliers

[29] Substitution of equation (11) in equation (8a) yields

$$\int_{\theta_L}^{\theta_u} \left\{ \frac{m-1}{m} [\lambda_* + \lambda_1 \theta] \right\}^{\frac{1}{m-1}} d\theta = 1 \quad (13)$$

Integration of equation (13) results in

$$(\lambda_* + \lambda_1 \theta_u)^{\frac{m}{m-1}} = \lambda_1 \left(\frac{m}{m-1} \right)^{\frac{m}{m-1}} + (\lambda_* + \lambda_1 \theta_L)^{\frac{m}{m-1}} \quad (14)$$

[30] Now substituting equation (11) in equation (8b), one gets

$$\int_{\theta_L}^{\theta_u} \theta \left\{ \frac{m-1}{m} [\lambda_* + \lambda_1 \theta] \right\}^{\frac{1}{m-1}} d\theta = \bar{\theta} \quad (15)$$

Integration of equation (15) leads to

$$\begin{aligned} \theta_u (\lambda_* + \lambda_1 \theta_u)^{\frac{m}{m-1}} + \left(\frac{m}{2m-1} \right) \frac{1}{\lambda_1} (\lambda_* + \lambda_1 \theta_L)^{\frac{2m-1}{m-1}} \\ - \theta_L (\lambda_* + \lambda_1 \theta_L)^{\frac{m}{m-1}} - \frac{1}{\lambda_1} \left(\frac{m}{2m-1} \right) (\lambda_* + \lambda_1 \theta_u)^{\frac{2m-1}{m-1}} \\ = \bar{\theta} \left[\lambda_1 \left(\frac{m}{m-1} \right)^{\frac{m}{m-1}} \right] \end{aligned} \quad (16)$$

Equations (14) and (16) contain two unknown Lagrange multipliers λ_* and λ_1 . These equations are nonlinear and can be solved numerically to obtain the value of Lagrange multipliers for given values of m , $\bar{\theta}$, θ_L , and θ_u .

[31] If $\theta_L = 0$, equation (14) simplifies to

$$(\lambda_* + \lambda_1 \theta_u)^{\frac{m}{m-1}} = \lambda_1 \left(\frac{m}{m-1} \right)^{\frac{m}{m-1}} + \lambda_*^{\frac{m}{m-1}} \quad (17)$$

Likewise equation (16) simplifies to

$$\begin{aligned} \theta_u (\lambda_* + \lambda_1 \theta_u)^{\frac{m}{m-1}} + \left(\frac{m}{2m-1} \right) \frac{1}{\lambda_1} (\lambda_*)^{\frac{2m-1}{m-1}} \\ - \frac{1}{\lambda_1} \left(\frac{m}{2m-1} \right) (\lambda_* + \lambda_1 \theta_u)^{\frac{2m-1}{m-1}} = \bar{\theta} \left[\lambda_1 \left(\frac{m}{m-1} \right)^{\frac{m}{m-1}} \right] \end{aligned} \quad (18)$$

Equation (17) and (18) can also be employed to determine the Lagrange multipliers λ_* and λ_1 for the simplified situation.

4.1.7. Soil Moisture Profile

[32] Coupling equations (11) and (7),

$$\left[\frac{m-1}{m} (\lambda_* + \lambda_1 \theta) \right]^{\frac{1}{m-1}} d\theta = -\frac{1}{L} dz \quad (19)$$

Integrating equation from $\theta = \theta_u$ to θ , and $z = 0$ to z , one gets

$$\theta = \frac{1}{\lambda_1} \left[\lambda_* + \lambda_1 \theta_u \right]^{\frac{m}{m-1}} - \frac{z}{L} \lambda_1 \left(\frac{m}{m-1} \right)^{\frac{m}{m-1}} - \frac{\lambda_*}{\lambda_1} \quad (20)$$

Equation (20) describes the moisture profile as a function of z for case 1, where the maximum soil moisture occurs at the surface and moisture decreases downward with increasing value of z .

4.2. Case 2: Dry Case

[33] The lowest moisture occurs at $z = 0$ and highest at $z = L$.

4.2.1. Specification of Hypothesis

[34] It is hypothesized that

$$F(\theta) = \frac{z}{L}, \quad f(\theta) = \frac{1}{L} \frac{dz}{d\theta} \quad (21)$$

4.2.2. Specification of Constraints

[35] The constraints for this case can be expressed as

$$\int_{\theta_u}^{\theta_L} f(\theta) d\theta = 1 \quad (22)$$

$$\int_{\theta_u}^{\theta_L} \theta f(\theta) d\theta = \bar{\theta} \quad (23)$$

4.2.3. Maximization of Entropy

[36] Following the same procedure as for case 1, the Lagrangian function L is obtained and is found to be the same as equation (9a).

4.2.4. Probability Density Function

[37] The entropy based probability distribution $f(\theta)$ for this case is found to be the same as equation (11).

4.2.5. Determination of the Lagrange Multipliers

[38] Substituting equation (11) in equation (22), one obtains

$$(\lambda_* + \lambda_1 \theta_L)^{\frac{m}{m-1}} - (\lambda_* + \lambda_1 \theta_u)^{\frac{m}{m-1}} = \lambda_1 \left(\frac{m}{m-1} \right)^{\frac{m}{m-1}} \quad (24)$$

Substituting equation (11) in equation (23), one obtains

$$\begin{aligned} \theta_L (\lambda_* + \lambda_1 \theta_L)^{\frac{m}{m-1}} - \theta_u (\lambda_* + \lambda_1 \theta_u)^{\frac{m}{m-1}} + \frac{1}{\lambda_1} \left(\frac{m}{2m-1} \right) \\ \cdot (\lambda_* + \lambda_1 \theta_u)^{\frac{2m-1}{m-1}} - \frac{1}{\lambda_1} \left(\frac{m}{2m-1} \right) (\lambda_* + \lambda_1 \theta_L)^{\frac{2m-1}{m-1}} \\ = \lambda_1 \left(\frac{m}{m-1} \right)^{\frac{m}{m-1}} \bar{\theta} \end{aligned} \quad (25)$$

Equation (24) and (25) can be employed to determine the unknown Lagrange multipliers λ_* and λ_1 .

[39] If $\theta_u = 0$, equations (24) and (25) simplify to

$$(\lambda_* + \lambda_1 \theta_L)^{\frac{m}{m-1}} = (\lambda_*)^{\frac{m}{m-1}} + \lambda_1 \left(\frac{m}{m-1} \right)^{\frac{m}{m-1}} \quad (26)$$

$$\begin{aligned} \theta_L (\lambda_* + \lambda_1 \theta_L)^{\frac{m}{m-1}} + \frac{1}{\lambda_1} \left(\frac{m}{2m-1} \right) (\lambda_*)^{\frac{2m-1}{m-1}} - \frac{1}{\lambda_1} \left(\frac{m}{2m-1} \right) \\ \cdot (\lambda_* + \lambda_1 \theta_L)^{\frac{2m-1}{m-1}} = \lambda_1 \left(\frac{m}{m-1} \right)^{\frac{m}{m-1}} \bar{\theta} \end{aligned} \quad (27)$$

Equations (26) and (27) can be employed to determine the Lagrange multipliers λ_* and λ_1 .

4.2.6. Soil Moisture Profile

[40] Substitution of equation (11) in equation (21) yields

$$\left[\frac{m-1}{m} (\lambda_* + \lambda_1 \theta) \right]^{\frac{1}{m-1}} d\theta = \frac{1}{L} dz \quad (28)$$

Solution of equation (28), subject to the condition that $\theta = \theta_u$ at $z = 0$ to $\theta = \theta$ at $z = z$, can be expressed as

$$\theta = \frac{1}{\lambda_1} \left[\frac{z}{L} \lambda_1 \left(\frac{m}{m-1} \right)^{\frac{m}{m-1}} + (\lambda_* + \lambda_1 \theta_u)^{\frac{m}{m-1}} \right]^{\frac{m-1}{m}} - \frac{\lambda_*}{\lambda_1} \quad (29a)$$

[41] If $\theta_u = 0$, equation (29a) reduces to

$$\theta = \frac{1}{\lambda_1} \left[\frac{z}{L} \lambda_1 \left(\frac{m}{m-1} \right)^{\frac{m}{m-1}} + (\lambda_*)^{\frac{m}{m-1}} \right]^{\frac{m-1}{m}} - \frac{\lambda_*}{\lambda_1} \quad (29b)$$

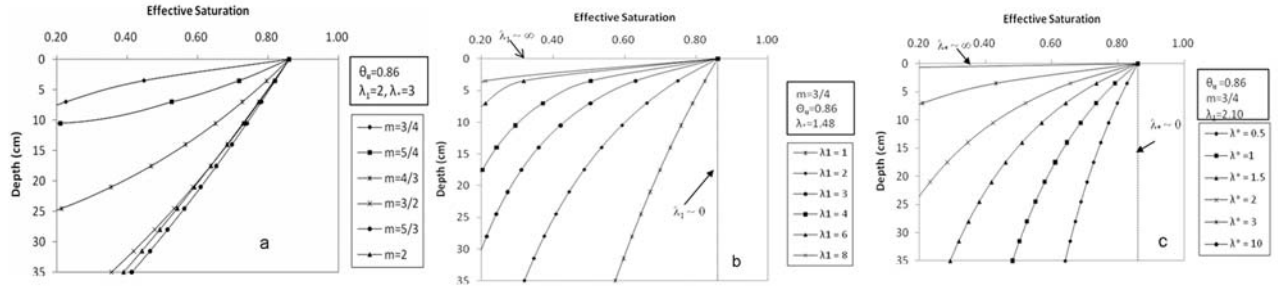


Figure 3. Soil moisture profiles for a wet case (a) for different values of m , (b) for different values of λ_1 , and (c) for different values of λ_* .

Equation (29a) yields the soil moisture profile as a function of z with parameters determined from equations (24) and (25) or equation (29b) for the simplified case with parameters determined from equations (26) and (27).

4.3. Case 3: Mixed Case

[42] This case can be considered to consist of two parts: Part I corresponding to the dry case and part II corresponding to the wet case. For part I, $0 \leq z \leq d$, the probability density function of θ , $f(\theta)$, is the same as in case 2 with the proviso that $\theta_u \leq \theta \leq \theta_d$, $\theta = \theta_d$ at $z = d$. Following the same steps as for case 2 (dry case), the moisture profile from equation (29a) becomes

$$\theta = \frac{1}{\lambda_1} \left[\lambda_* + \lambda_1 \theta_u \right]^{\frac{m}{m-1}} + \frac{z}{d} \lambda_1 \left(\frac{m}{m-1} \right)^{\frac{m}{m-1}} - \frac{\lambda_*}{\lambda_1} \quad (30)$$

Equation (30) contains the unknown Lagrange multipliers λ_* and λ_1 which can be determined using the modified form of constraints given by equations (22) and (23):

$$\int_{\theta_u}^{\theta_d} f(\theta) d\theta = 1 \quad (31a)$$

$$\int_{\theta_u}^{\theta_d} \theta f(\theta) d\theta = \overline{\theta_{up}} \quad (31b)$$

where

$$\overline{\theta_{up}} = \frac{1}{d} \int_0^d \theta(z) dz \quad (31c)$$

Now substituting equation (11) in equation (31a), one gets

$$\int_{\theta_u}^{\theta_d} \left[\frac{m-1}{m} (\lambda_* + \lambda_1 \theta) \right]^{\frac{1}{m-1}} d\theta = 1 \quad (32a)$$

Integration of equation (32a) yields

$$(\lambda_* + \lambda_1 \theta_d)^{\frac{m}{m-1}} - (\lambda_* + \lambda_1 \theta_u)^{\frac{m}{m-1}} = \lambda_1 \left(\frac{m}{m-1} \right)^{\frac{m}{m-1}} \quad (32b)$$

Substitution of equation (12) in equation (31b) yields

$$\int_{\theta_u}^{\theta_d} \theta \left[\left(\frac{m-1}{m} \right) (\lambda_* + \lambda_1 \theta) \right]^{\frac{1}{m-1}} d\theta = \overline{\theta_{up}} \quad (33a)$$

Solution of equation (33) yields

$$\begin{aligned} & \theta_d (\lambda_* + \lambda_1 \theta_d)^{\frac{m}{m-1}} - \theta_u (\lambda_* + \lambda_1 \theta_u)^{\frac{m}{m-1}} + \frac{1}{\lambda_1} \left(\frac{m}{2m-1} \right) \\ & \cdot (\lambda_* + \lambda_1 \theta_u)^{\frac{2m-1}{m-1}} - \frac{1}{\lambda_1} \left(\frac{m}{2m-1} \right) (\lambda_* + \lambda_1 \theta_d)^{\frac{2m-1}{m-1}} \\ & = \lambda_1 \left(\frac{m}{m-1} \right)^{\frac{m}{m-1}} \overline{\theta_{up}} \end{aligned} \quad (33b)$$

Equations (33a) and (33b) are solved to obtain the unknown Lagrange multipliers λ_* and λ_1 given the values of m , θ_u , and $\overline{\theta_{up}}$. Note that θ_d is common between the two parts so it is estimated by matching the soil moisture profiles for the two cases at $z = d$.

[43] For part II (corresponding to the wet case), $d \leq z \leq L$. The moisture profile can be expressed from equation (20). Note that the hypothesis expressed by equation (7) is valid

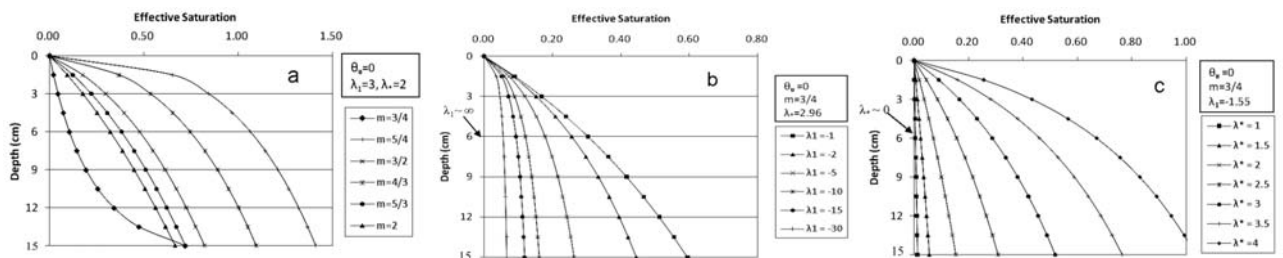


Figure 4. Soil moisture profiles for a dry case (a) for different values of m , (b) for different values of λ_1 , and (c) for different values of λ_* .

Table 1. Parameter Estimation for Four Sets of Data From *Melone et al.* [2006] for Wet Case^a

| θ_u | θ_m | θ_L | λ_1 | λ_* | m | Data Source |
|------------|------------|------------|-------------|-------------|-----|-------------|
| 0.860 | 0.543 | 0.000 | -1.388 | 3.585 | 3/4 | SME 1 |
| 0.453 | 0.427 | 0.416 | 24.341 | 9.142 | 3/4 | SME 2 |
| 0.471 | 0.232 | 0.086 | -2.314 | 1.787 | 3/4 | SME 3 |
| 0.432 | 0.263 | 0.080 | -0.392 | 2.413 | 3/4 | SME 4 |

^aNotation: θ_u , soil moisture at $z = 0$; θ_m , mean soil moisture; θ_L , soil moisture at $z = L$; λ_1 , first Lagrange multiplier; λ_* , modified zeroth Lagrange multiplier; m , exponent.

over $L - d$, wherein L is replaced by $L - d$ and z by $z - d$. Using equation (20) one gets

$$\theta = \frac{1}{\lambda_1} \left[\frac{d - z}{L - d} \left(\frac{m}{m - 1} \right)^{\frac{m}{m - 1}} \frac{1}{\lambda_1} + (\lambda_* + \lambda_1 \theta_d)^{\frac{m}{m - 1}} \right] - \frac{\lambda_*}{\lambda_1} \quad (34)$$

Equation (34) has two unknown Lagrange multipliers which can be determined by modifying the constraints for this case expressed by equations (8a) and (8b) as follows:

$$\int_{\theta_L}^{\theta_d} f(\theta) d\theta = 1 \quad (35a)$$

$$\int_{\theta_L}^{\theta_d} \theta f(\theta) d\theta = \overline{\theta_{Low}} \quad (35b)$$

where

$$\overline{\theta_{Low}} = \frac{1}{L - d} \int_d^L \theta(z) dz \quad (35c)$$

Substitution of equation (11) in equation (35a), with the condition that at $z = d$, $\theta = \theta_d$, and $z = L$, $\theta = \theta_L$, yields

$$\int_{\theta_L}^{\theta_d} \left[\frac{m - 1}{m} (\lambda_* + \lambda_1 \theta) \right]^{\frac{1}{m - 1}} d\theta = 1 \quad (36a)$$

This leads to

$$(\lambda_* + \lambda_1 \theta_d)^{\frac{m}{m - 1}} - (\lambda_* + \lambda_1 \theta_L)^{\frac{m}{m - 1}} = \lambda_1 \left(\frac{m}{m - 1} \right)^{\frac{m}{m - 1}} \quad (36b)$$

Table 2. Parameter Estimation for Four Sets of Data for Dry Case^a

| θ_L | θ_m | θ_u | λ_1 | λ_* | m | Data Source |
|------------|------------|------------|-------------|-------------|-----|-------------|
| 0.250 | 0.210 | 0.100 | 10.246 | 3.895 | 3/4 | USDA EXP 1 |
| 0.260 | 0.230 | 0.170 | -9.864 | 3.859 | 3/4 | USDA EXP 2 |
| 0.775 | 0.374 | 0.130 | 1.584 | 2.050 | 3/4 | SME 1 |
| 0.465 | 0.394 | 0.322 | -0.135 | 1.898 | 3/4 | SME 2 |

^aNotation: θ_u , soil moisture at $z = 0$; θ_m , mean soil moisture; θ_L , soil moisture at $z = L$; λ_1 , first Lagrange multiplier; λ_* , modified zeroth Lagrange multiplier; m , exponent.

Table 3. Parameter Estimation for Four Sets of Data for Mixed Case^a

| θ_u | θ_{m-I} | θ_d | λ_1 | λ_* | m | Data Source |
|------------|-----------------|------------|-------------|-------------|-----|-------------|
| 0.351 | 0.364 | 0.417 | -28.375 | 8.989 | 3/4 | SME 1 |
| θ_u | θ_{m-II} | θ_L | λ_1 | λ_* | m | SME 1 |
| 0.417 | 0.340 | 0.337 | 104.621 | 34.621 | 3/4 | SME 1 |
| 0.379 | 0.404 | 0.428 | -0.882 | 1.768 | 3/4 | SME 2 |
| θ_d | θ_{m-II} | θ_L | λ_1 | λ_* | m | SME 2 |
| 0.428 | 0.335 | 0.330 | -70.748 | 22.622 | 3/4 | SME 2 |
| 0.334 | 0.369 | 0.410 | -2.465 | -0.663 | 3/4 | SME 3 |
| θ_d | θ_{m-II} | θ_L | λ_1 | λ_* | m | SME 3 |
| 0.410 | 0.278 | 0.080 | -2.123 | 2.838 | 3/4 | SME 3 |

^aNotation: θ_u , soil moisture at $z = 0$; θ_{m-I} , mean moisture content for data set I; θ_{m-II} , mean moisture content for data set II; θ_L , soil moisture at $z = L$; λ_1 = first Lagrange multiplier; λ_* , modified zeroth Lagrange multiplier; m , exponent.

Likewise, substituting equation (11) in equation (35b) one obtains

$$\begin{aligned} & \theta_d (\lambda_* + \lambda_1 \theta_d)^{\frac{m}{m - 1}} - \theta_L (\lambda_* + \lambda_1 \theta_L)^{\frac{m}{m - 1}} + \frac{1}{\lambda_1} \left(\frac{m}{2m - 1} \right) \\ & \cdot (\lambda_* + \lambda_1 \theta_L)^{\frac{2m - 1}{m - 1}} - \frac{1}{\lambda_1} \left(\frac{m}{2m - 1} \right) (\lambda_* + \lambda_1 \theta_d)^{\frac{2m - 1}{m - 1}} \\ & = \lambda_1 \left(\frac{m}{m - 1} \right)^{\frac{m}{m - 1}} \overline{\theta_{Low}} \end{aligned} \quad (36c)$$

Equations (36a) and (36b) are nonlinear and are therefore to be solved numerically for λ_1 and λ_* .

5. Testing of the Theory

[44] Equation (12) gives the probability density function of the soil moisture content, in which the probability density for any value of moisture content must always be positive. Therefore, $\lambda_* + \lambda_1 \theta < 0$ or for $\theta < -\lambda_*/\lambda_1$. This shows that if one parameter is positive then the other

Table 4. Computed and Observed Soil Moisture Profiles for Wet Case

| Depth (cm) | Observed θ | Computed θ | Relative Error (%) |
|------------------------|-------------------|-------------------|--------------------|
| <i>SME 1: Wet Case</i> | | | |
| 15 | 0.860 | 0.860 | 0.000 |
| 25 | 0.803 | 0.700 | 0.128 |
| 35 | 0.509 | 0.460 | 0.096 |
| 45 | 0.000 | 0.000 | 0.000 |
| <i>SME 2: Wet Case</i> | | | |
| 10 | 0.453 | 0.450 | 0.007 |
| 20 | 0.447 | 0.440 | 0.016 |
| 30 | 0.400 | 0.430 | -0.075 |
| 45 | 0.420 | 0.420 | 0.000 |
| 60 | 0.416 | 0.420 | -0.010 |
| <i>SME 3: Wet Case</i> | | | |
| 10 | 0.471 | 0.470 | 0.002 |
| 20 | 0.443 | 0.340 | 0.233 |
| 30 | 0.277 | 0.250 | 0.097 |
| 45 | 0.083 | 0.083 | 0.000 |
| 60 | 0.086 | 0.086 | 0.000 |
| <i>SME 4: Wet Case</i> | | | |
| 10 | 0.432 | 0.430 | 0.005 |
| 20 | 0.386 | 0.370 | 0.041 |
| 30 | 0.336 | 0.300 | 0.107 |
| 45 | 0.080 | 0.190 | -1.375 |
| 60 | 0.080 | 0.080 | 0.000 |

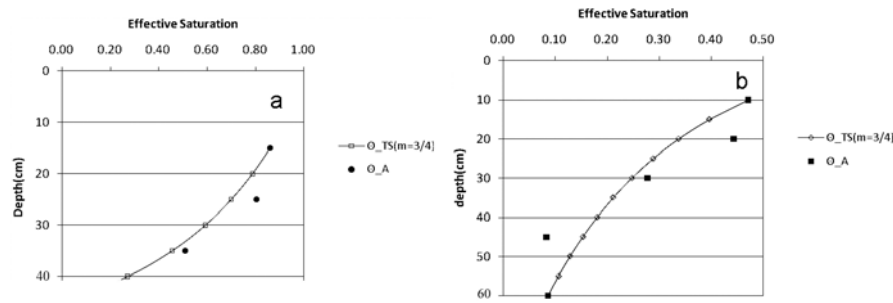


Figure 5. Soil moisture profiles for wet cases for (a) SME 1 and (b) SME 3. Here θ_A is observed (or actual) moisture content and θ_{TS} is moisture content computed using the Tsallis entropy with exponent $m = 3/4$.

parameter must be proportionately negative in order to ensure the positivity of the probability density function values. Likewise, equation (11) yields the Tsallis entropy of the moisture content. The entropy will be positive if $(\lambda_* + \lambda_1 \bar{\theta}) > m/(m - 1)$.

5.1. Variation in Soil Moisture Profiles With Variation in Parameters

[45] It may be interesting to investigate how the soil moisture profiles for wet (equation (20) or its simplification given by equation (18)), dry (equation (29) or its simplification) and mixed (equations (30) and (34)) cases vary with changes in parameters: m , λ_1 , and λ_* . Soil moisture profiles as a function of z were computed for the three cases by varying one parameter at a time. For the wet (case 1), Figure 3a shows soil moisture profiles for different values of the m parameter, Figure 3b for different values of λ_1 , and Figure 3c for different values of λ_* . It is seen that the moisture profile is quite sensitive to these parameters. For m equal to or exceeding $3/2$, the moisture profile does not change significantly. For these values of m and up to $m = 5/4$, the profile is concave to the θ axis and then for $m < 1$, its shape changes and becomes convex. This is because of the nature of the nonlinear equation of the soil moisture profile. Extensive testing showed that $m = 3/4$ was more realistic and yielded better moisture profiles and hence the value of m was fixed at 0.75 . For extreme values of λ_1 the moisture profile becomes a straight line as shown in Figure 3b. The value of parameter λ_1 can take on both

positive and negative values. In between these extremes, the moisture profile is curved-convex to the horizontal axis. The same is found for parameter λ_* (as shown in Figure 6). The value of this parameter is usually positive.

[46] For the dry case, the moisture profiles as a function of z are shown in Figure 4a for different values of m , in Figure 4b for different values of λ_1 and in Figure 4c for different values of λ_* . It is interesting to note that the shape of moisture profiles for different values of m is opposite to that in the wet case. This is also true for the shapes of soil moisture profiles for different values of λ_1 and λ_* . The value of parameter λ_* remains positive but λ_1 can take on both negative and positive values.

5.2. Experimental Observations

[47] Melone *et al.* [2006] reported experimental data on loam soil, and sandy clay loam. Experiments were conducted using a soil tray 152 cm long, 122 cm wide, and 78 cm deep. Beneath the bottom of the soil column, a 7 cm deep gravel layer was provided to allow for the outflow of percolated water. Experiments started on a uniform soil

Table 5. Computed and Observed Soil Moisture Profiles for Dry Case

| Depth (cm) | Observed θ | Computed θ | Relative Error (%) |
|--------------|-------------------|-------------------|--------------------|
| <i>SME 1</i> | | | |
| 10 | 0.130 | 0.130 | 0.000 |
| 15 | 0.175 | 0.180 | -0.029 |
| 20 | 0.220 | 0.240 | -0.091 |
| 25 | 0.293 | 0.300 | -0.024 |
| 35 | 0.650 | 0.480 | 0.262 |
| 45 | 0.775 | 0.770 | 0.006 |
| <i>SME 2</i> | | | |
| 10 | 0.32 | 0.33 | -0.04 |
| 20 | 0.38 | 0.40 | -0.06 |
| 30 | 0.40 | 0.41 | -0.04 |
| 45 | 0.41 | 0.44 | -0.09 |
| 60 | 0.47 | 0.45 | 0.03 |

Table 6. Computed and Observed Soil Moisture Profiles for Dry Case Long After Rainfall Using USDA Experimental Data

| Depth (m) | Observed θ | Computed θ | Relative error (%) |
|-------------------|-------------------|-------------------|--------------------|
| <i>USDA EXP 1</i> | | | |
| 0 | 0.100 | 0.100 | 0.000 |
| 0.08 | 0.130 | 0.141 | -0.081 |
| 0.18 | 0.180 | 0.169 | 0.059 |
| 0.28 | 0.200 | 0.188 | 0.061 |
| 0.42 | 0.190 | 0.206 | -0.083 |
| 0.48 | 0.220 | 0.212 | 0.038 |
| 0.58 | 0.230 | 0.220 | 0.044 |
| 0.68 | 0.230 | 0.227 | 0.014 |
| 0.8 | 0.230 | 0.234 | -0.016 |
| 0.88 | 0.240 | 0.238 | 0.010 |
| 1 | 0.240 | 0.243 | -0.011 |
| 1.08 | 0.250 | 0.246 | 0.017 |
| 1.2 | 0.250 | 0.250 | 0.000 |
| <i>USDA EXP 2</i> | | | |
| 0.08 | 0.170 | 0.186 | -0.096 |
| 0.22 | 0.210 | 0.206 | 0.018 |
| 0.38 | 0.230 | 0.222 | 0.036 |
| 0.52 | 0.240 | 0.232 | 0.034 |
| 0.68 | 0.240 | 0.241 | -0.004 |
| 0.84 | 0.250 | 0.248 | 0.007 |
| 1 | 0.260 | 0.254 | 0.022 |
| 1.18 | 0.260 | 0.260 | 0.000 |

Table 7. Computed and Observed Soil Moisture Profiles for Mixed Case

| Depth (cm) | Observed θ | Computed θ | Relative Error (%) |
|--------------|-------------------|-------------------|--------------------|
| <i>SME 1</i> | | | |
| 10 | 0.351 | 0.351 | 0.00 |
| 20 | 0.417 | 0.417 | 0.00 |
| 30 | 0.341 | 0.346 | -0.01 |
| 45 | 0.338 | 0.338 | 0.00 |
| 60 | 0.337 | 0.337 | 0.00 |
| <i>SME 2</i> | | | |
| 10 | 0.379 | 0.379 | 0.000 |
| 20 | 0.428 | 0.428 | 0.000 |
| 30 | 0.340 | 0.336 | 0.012 |
| 45 | 0.336 | 0.332 | 0.012 |
| 60 | 0.330 | 0.330 | 0.000 |
| <i>SME 3</i> | | | |
| 10 | 0.334 | 0.334 | 0.000 |
| 20 | 0.404 | 0.410 | -0.015 |
| 30 | 0.410 | 0.359 | 0.124 |
| 45 | 0.344 | 0.253 | 0.265 |
| 60 | 0.080 | 0.080 | 0.000 |

moisture content and under uniform rainfall. For sandy clay loam soil, rainfall = 2.4 cm/h for 8 h, $K = 2.1$ cm/h, $n = 0.485$, $\theta_0 = 0.043$, $ET = 0$, and no lateral runoff. Therefore, the accumulated rainfall w was = 2.4, 4.8, 7.2, 9.6, 12, 14.4, 16.8, and 19.2 cm at $t = 1, 2, 3, 4, 5, 6, 7$, and 8 h, respectively. The value of $L = 55$ cm = the effective soil column depth during the rainfall event. After the rainfall event, $w = 19.2$ cm during the time of redistribution of soil moisture, assuming no deep percolation. From these reported data, four sets of data for the wet case (labeled as Soil Moisture Experiments (SME) 1, 2, 3, and 4), two sets of data for the dry case (labeled as Soil Moisture Experiments (SME) 1, and 2) and three sets of data for the mixed case (labeled as Soil Moisture Experiments (SME) 1, 2, and 3) were extracted. In addition, two sets of experimental data on soil moisture for the dry case were obtained from *Heathman* [1992, 1994] published by the U.S. Department of Agriculture. The measurements were made using a Resonant Frequency Capacitance (RFC) probe 15.24 cm (6 inch) intervals to a depth of 114.3 cm (45 inches) beginning at 7.62 cm (3 inches) below the soil surface. These data sets were labeled as USDA Experiment (EXP) 1 and 2. In all there were eleven data sets and these were used for determining parameters and testing the entropy theory.

5.3. Parameter Estimation

[48] In order to construct soil moisture profiles, values of θ at the soil surface (upper boundary condition), θ_u ; the value at the lower boundary, θ_L ; and the average value $\bar{\theta}$ need to be specified. Also need to be specified are the initial soil moisture content θ_0 , soil porosity n , and the location of the lower boundary or the depth d of the soil column. These moisture values were obtained from the observations of soil moisture content. For both wet and dry cases, values of θ_u , θ_L , and θ_m were obtained from observations for each experimental data set, as given in Table 1. Then, values of parameters, Lagrange multipliers, λ_1 and λ_* were obtained by fitting soil moisture profile equations to experimental data sets and are shown in Tables 1 and 2. For the mixed case, values of θ_u , θ_d , and θ_m were obtained from observations. Values of parameters λ_1 and λ_* are shown in Table 3.

5.4. Computation of Soil Moisture Profiles

[49] Soil moisture profiles were computed using equation (20) with $m = 0.75$ for each data set for the wet case. The relative error between observed and computed soil moisture values were also computed for all four data sets and these are shown in Table 4. For two sample data sets the profiles are shown in Figures 5a and 5b. The relative error was less than 13% for SME 1, less than 1% for SME 2, less than 24% for SME 3, and less than 138% for SME 4. In each case there was just one value of moisture content that was not captured well. This may be either due to experimental observation error or errors in parameter values.

[50] For the dry case, computed and observed soil moisture values are shown in Tables 5 and 6. For two sample data sets computed and observed soil moisture profiles are shown in Figures 6a and 6b. The relative error was less than 27% for SME 1, less than 1% for SME 2, less than 9% for USDA-EXP 1 and less than 4% for USDA-EXP 2. Overall, the computed soil moistures were in good agreement with the observed profiles.

[51] For the mixed case, computed and observed soil moisture values are shown in Table 7. For two sample data sets computed and observed soil moisture profiles are shown in Figures 7a and 7b. The relative error was less than 2% for SME 1, and less than 27% for SME 2. The computed soil moisture profiles were in good agreement with the observed profiles.

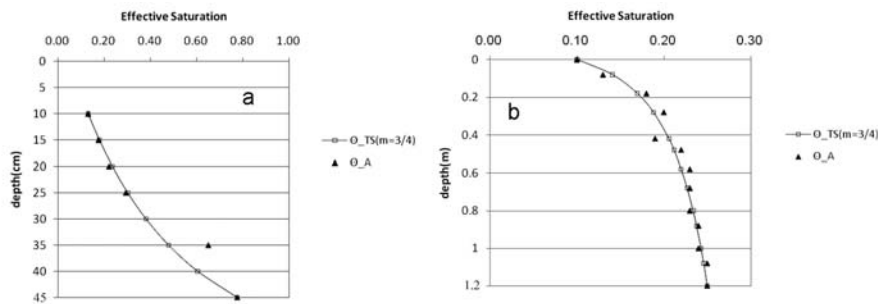


Figure 6. Soil moisture profile for (a) SME 1 and (b) USDA EXP I for dry cases. Here θ_A is observed (or actual) moisture content and θ_{TS} is moisture content computed using the Tsallis entropy with exponent $m = 3/4$.

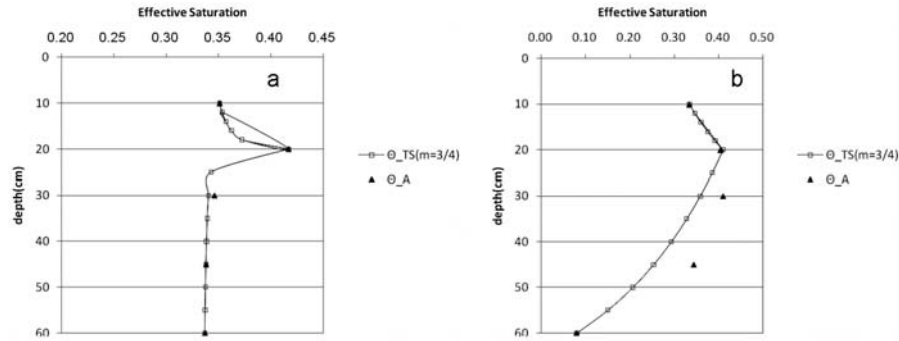


Figure 7. Soil moisture profiles for mixed cases (a) for SME I and (b) for SME 3. Here θ_A is observed (or actual) moisture content and θ_{TS} is moisture content computed using the Tsallis entropy with exponent $m = 3/4$.

5.5. Practical Application

[52] The proposed entropy theory-based soil moisture profiles can be incorporated in watershed hydrologic modeling. To that end, in addition to parameters λ_1 and λ_* , values of d and θ_m need to be determined. The value of d can be obtained using an infiltration model or a kinematic wave model requiring only the value of soil moisture at the surface. Following Singh [1997] and Singh and Joseph [1994], this depth can be computed as

$$d = \frac{K}{\theta_u} t \quad (37)$$

where K is the hydraulic conductivity (treated as parameter), and t is time the wetting front takes to travel the distance d .

[53] The mean value of θ , θ_m , can be calculated using a water balance method, discussed by Al-Hamdan and Cruise [2010], as

$$\bar{\theta} = \frac{w/(nL)}{n - \theta_0} \quad (38)$$

where w is the water applied to the soil surface and can be computed considering the water balance for any time step as

$$w = w_{5i-1} - w_{5i} + P_i + \Delta R - ET \quad (39)$$

where all quantities are measured in units of depth, i is the time step, $i - 1$ is the previous time step, w is the water depth applied to the soil within a time step, w_5 is the water content (in units of depth) for the 5 cm deep surface (which can be measured by say remote sensing), P is the amount of precipitation (in units of depth), ET is the amount of evapotranspiration (in units of depth), and ΔR is the difference between the amount of runoff leaving a particular soil area and the amount entering that soil area cell (in units of depth). The values of θ_u and θ_L must also be specified.

6. Conclusions

[54] The following conclusions are drawn from this study.

[55] 1. The entropy theory seems capable of simulating soil moisture profiles for wet, dry and mixed cases reasonably well.

[56] 2. Parameters of the theory can be determined from observations.

[57] 3. More testing is needed to test the theory and regionalize its parameters.

[58] **Acknowledgments.** The author would like to express his sincere gratitude to three anonymous reviewers for their constructive comments. Inclusion of these comments has resulted in an improved manuscript. Luo Hao, a graduate student in the Department of Biological and Agricultural Engineering at Texas A&M University helped with computation and construction of graphs in the paper, and her help is gratefully acknowledged. The work reported in the paper was supported in part by the United States Geological Survey and Texas Water Resources Research Institute through the project "Hydrological Drought Characterization for Texas under Climate Change, with Implications for Water Resources Planning and Management" (USGS, project 2009TX334G).

References

- Abe, S., and G. B. Bagci (2005), Necessity of q -expectation value in non-extensive statistical mechanics, *Phys. Rev. E*, **71**, 016139, doi:10.1103/PhysRevE.71.016139.
- Al-Hamdan, O. Z., and J. F. Cruise (2010), Soil moisture profile development from surface observations by principle of maximum entropy, *J. Hydrol. Eng.*, in press.
- Arimitsu, N., and T. Arimitsu (2002a), PDF of velocity fluctuation in turbulence by a statistics based on generalized entropy, *Physica A*, **305**, 218–226, doi:10.1016/S0378-4371(01)00665-3.
- Arimitsu, N., and T. Arimitsu (2002b), Analysis of velocity derivatives in turbulence based on generalized statistics, *Europhys. Lett.*, **60**(1), 60–67, doi:10.1209/epl/2002-00318-5.
- Arya, L. M., J. C. Richter, and J. F. Paris (1983), Estimating profile water storage from surface zone soil moisture measurements under bare field conditions, *Water Resour. Res.*, **19**(2), 403–412, doi:10.1029/WR019i002p00403.
- Assouline, S., D. Tessier, and A. Bruand (1998), A conceptual model of the soil water retention curve, *Water Resour. Res.*, **34**(2), 223–231, doi:10.1029/97WR03039.
- Boghosian, B. M. (1996), Thermodynamic description of the relaxation of two-dimensional turbulence using Tsallis statistics, *Phys. Rev. E*, **53**(5), 4754–4763, doi:10.1103/PhysRevE.53.4754.
- Boon, J.-P., and C. Tsallis (Eds.) (2005), *Nonextensive Statistical Mechanics—New Trends, New Perspectives*, *Europhys. News*, **36**(6), 185–231.
- Bruckler, L., H. Witono, and P. Stengel (1988), Near surface soil moisture estimation from microwave measurements, *Remote Sens. Environ.*, **26**, 101–121, doi:10.1016/0034-4257(88)90091-0.
- Costa, U. M. S., M. L. Lyra, A. R. Plastino, and C. Tsallis (1997), Power-law sensitivity to initial conditions within a logisticlike family of maps: Fractality and nonextensivity, *Phys. Rev. E*, **56**(1), 245–250, doi:10.1103/PhysRevE.56.245.
- Das, N. N., and B. P. Mohanty (2006), Rootzone soil moisture assessment using remote sensing and vadose zone modeling, *Vadose Zone J.*, **5**, 296–307, doi:10.2136/vzj2005.0033.
- De Troch, F. P., P. A. Troch, Z. Su, and D. S. Lin (1996), Application of remote sensing for hydrological modeling, in *Distributed Hydrological*

- Modeling*, edited by M. B. Abbott and J. Refsgaard, pp. 165–191, Kluwer Acad., Dordrecht, Netherlands.
- Gotoh, T., and R. H. Kraichnan (2004), Turbulence and Tsallis statistics, *Physica D*, 193, 231–244, doi:10.1016/j.physd.2004.01.034.
- Heathman, G. C. (1992), Data report: Profile soil moisture, U.S. Dep. of Agric., Washington, D. C.
- Heathman, G. C. (1994), Data report: Profile soil moisture, U.S. Dep. of Agric., Washington, D. C.
- Jackson, T. J., M. E. Hawley, and P. E. O'Neill (1987), Preplanting soil moisture using passive microwave sensors, *Water Resour. Bull.*, 23(1), 11–19.
- Jain, S. K., V. P. Singh, and M. T. van Genuchten (2004), Analysis of soil water retention data using artificial neural networks, *J. Hydrol. Eng.*, 9(5), 415–420, doi:10.1061/(ASCE)1084-0699(2004)9:5(415).
- Jaynes, E. T. (1957a), Information theory and statistical mechanics I, *Phys. Rev.*, 106(4), 620–630, doi:10.1103/PhysRev.106.620.
- Jaynes, E. T. (1957b), Information theory and statistical mechanics II, *Phys. Rev.*, 108(2), 171–190, doi:10.1103/PhysRev.108.171.
- Keylock, C. J. (2005), Describing the recurrence interval of extreme floods using nonextensive thermodynamics and Tsallis statistics, *Adv. Water Resour.*, 28, 773–778, doi:10.1016/j.advwatres.2005.02.011.
- Koekoek, E. J. W., and H. Boeltink (1999), Neural network models to predict soil water retention, *Eur. J. Soil Sci.*, 50, 489–495, doi:10.1046/j.1365-2389.1999.00247.x.
- Kondratyev, K. Y., V. V. Melentyev, Y. I. Rabinovich, and E. M. Shulgina (1977), Passive microwave remote sensing of soil moisture, paper presented at 11th Symposium on Remote Sensing of the Environment, Environ. Res. Inst. of Mich., Ann Arbor.
- Kostov, K. G., and T. J. Jackson (1993), Estimating profile soil moisture from surface layer measurements—A review, *Proc. Int. Soc. Opt. Eng.*, 1941, 125–136.
- Koutsoyiannis, D. (2005a), Uncertainty, entropy, scaling and hydrological stochasticity. 1. Marginal distributional properties of hydrological processes and state scaling, *Hydrol. Sci. J.*, 50(3), 381–404, doi:10.1623/hysj.50.3.381.65031.
- Koutsoyiannis, D. (2005b), Uncertainty, entropy, scaling and hydrological stochasticity. 2. Time dependence of hydrological processes and state scaling, *Hydrol. Sci. J.*, 50(3), 405–426, doi:10.1623/hysj.50.3.405.65028.
- Lyra, M. L., and C. Tsallis (1998), Nonextensivity and multifractality in low-dimensional dissipative systems, *Phys. Rev. Lett.*, 80(1), 53–56, doi:10.1103/PhysRevLett.80.53.
- Melone, F., C. Corradini, R. Morbidelli, and C. Saltalippi (2006), Laboratory experimental check of a conceptual model for infiltration under complex patterns, *Hydrol. Processes*, 20, 439–452, doi:10.1002/hyp.5913.
- Or, D., F. J. Leij, V. Snyder, and A. Ghezzehei (2000), Stochastic model for posttillage soil pore space evolution, *Water Resour. Res.*, 36(7), 1641–1652, doi:10.1029/2000WR900092.
- Pachepsky, Y., A. Guber, D. Jacques, J. Simunek, M. T. V. Genuchten, T. Nicholson, and R. Cady (2006), Information content and complexity of simulated soil water fluxes, *Geoderma*, 134(3–4), 253–266, doi:10.1016/j.geoderma.2006.03.003.
- Papa, A. R. R., and C. Tsallis (1998), Imitation games: Power-law sensitivity to initial conditions and nonextensivity, *Phys. Rev. E*, 57(4), 3923–3927, doi:10.1103/PhysRevE.57.3923.
- Prato, D., and C. Tsallis (1999), Nonextensive foundation of levy distributions, *Phys. Rev. E*, 60(2), 2398–2401, doi:10.1103/PhysRevE.60.2398.
- Reutov, E. A., and A. M. Shutko (1986), Prior-knowledge based soil moisture determination of microwave radiometry, *Sov. J. Remote Sensing*, 5(1), 100–125.
- Russo, D. (1988), Determining soil hydraulic properties by parameter estimation: On the selection of a model for the hydraulic properties, *Water Resour. Res.*, 24(3), 453–459, doi:10.1029/WR024i003p00453.
- Schmugge, T. J., T. J. Jackson, and H. L. McKim (1980), Survey of methods for soil moisture determination, *Water Resour. Res.*, 16(6), 961–979, doi:10.1029/WR016i006p00961.
- Singh, V. P. (1989), *Hydrologic Systems*, vol. 2, *Watershed Modeling*, Prentice Hall, Englewood Cliffs, N. J.
- Singh, V. P. (1997), *Kinematic Wave Modeling in Water Resources: Environmental Hydrology*, John Wiley, New York.
- Singh, V. P., and E. Joseph (1994), Kinematic wave model for soil moisture movement with plant root extraction, *Irrig. Sci.*, 14, 189–198, doi:10.1007/BF00190190.
- Srivastava, S. K., N. Yograjan, V. Jayaraman, P. P. Nageswara, and M. G. Chandrasekhar (1997), On the relationship between ERS-1 SAR/backscatter and surface/subsurface soil moisture variations in vertisols, *Acta Astronaut.*, 40(10), 693–699, doi:10.1016/S0094-5765(97)00125-2.
- Tsallis, C. (1988), Possible generalization of Boltzmann-Gibbs statistics, *J. Stat. Phys.*, 52(1–2), 479–487, doi:10.1007/BF01016429.
- Tsallis, C. (2002), Entropic nonextensivity: A possible measure of complexity, *Chaos Solitons Fractals*, 13, 371–391, doi:10.1016/S0960-0779(01)00019-4.
- Tsallis, C. (2004), Nonextensive statistical mechanics: Construction and physical interpretation, in *Nonextensive Entropy-Interdisciplinary Applications*, edited by M. Gell-Mann and C. Tsallis, pp. 1–52, Oxford Univ. Press, New York.
- Tsallis, C., and D. J. Bukman (1996), Anomalous diffusion in the presence of external forces: Exact time-dependent solutions and their thermodynamical basis, *Phys. Rev. E*, 54(3), R2197–R2200, doi:10.1103/PhysRevE.54.R2197.
- Tsallis, C., R. S. Mendes, and A. R. Plastino (1998), The role of constraints within generalized nonextensive statistics, *Physica A*, 261, 534–554, doi:10.1016/S0378-4371(98)00437-3.
- Ulaby, F. T., P. C. Dubois, and J. V. Zyl (1996), Radar mapping of surface soil moisture, *J. Hydrol.*, 184, 57–84, doi:10.1016/0022-1694(95)02968-0.
- Zanette, D. H., and P. Alemany (1995), Thermodynamics of anomalous diffusion, *Phys. Rev. Lett.*, 75(3), 366–369, doi:10.1103/PhysRevLett.75.366.

V. P. Singh, Department of Biological and Agricultural Engineering, Texas A&M University, College Station, TX 77843-2117, USA. (vsingh@tamu.edu)